The Astrophysical Journal Letters, 997:L9 (9pp), 2026 January 20 https://doi.org/10.3847/2041-8213/ae2c73

First Associated Neutrino Search for a Failed Supernova Candidate with Super-Kamiokande

F. Nakanishi[1], K. Abe[2,3], S. Abe[2], Y. Asaoka[2], M. Harada[2], Y. Hayato[2,3], K. Hiraide[2,3], K. Hosokawa[2], T. H. Hung[2], K. Ieki[2,3], M. Ikeda[2,3], J. Kameda[2,3], Y. Kanemura[2], Y. Kataoka[2,3], S. Miki[2], S. Mine[2,4], M. Miura[2,3], S. Moriyama[2,3], M. Nakahata[2,2,3], S. Nakayama[2,3], Y. Noguchi[2], G. Pronost[2], K. Sato[2], H. Sekiya[2,3], M. Shiozawa[2,3], Y. Suzuki[2], A. Takeda[2,3], Y. Takemoto[2,3], H. Tanaka[2,3], T. Yano[2], Y. Itow[5,6,7], T. Kajita[3,5,8], R. Nishijima[5], K. Okumura[3,5], T. Tashiro[5], T. Tomiya[5], X. Wang[5], P. Fernandez[9], L. Labarga[9], B. Zaldivar[9], B. W. Pointon[10,11], C. Yanagisawa[12,13], E. Kearns[3,14], L. Wan[14], T. Wester[14], J. Bian[4], B. Cortez[4], N. J. Griskevich[4], Y. Jiang[4], M. B. Smy[3,4], H. W. Sobel[3,4], V. Takhistov[4,15], A. Yankelevich[4], J. Hill[16], M. C. Jang[17], S. H. Lee[17], D. H. Moon[17], R. G. Park[17], B. S. Yang[17], B. Bodur[18], K. Scholberg[3,18], C. W. Walter[3,18], A. Beauchêne[19], Le Blévec[19], O. Drapier[19], A. Ershova[19], M. Ferey[19], Th. A. Mueller[19], A. D. Santos[19], P. Paganini[19], C. Quach[19], R. Rogly[19], T. Nakamura[20], J. S. Jang[21], R. P. Litchfield[22], L. N. Machado[22], F. J. .P Soler[22], J. G. Learned[23], K. Choi[24], S. Cao[25], L. H. V. Anthony[26], N. W. Prouse[26], M. Scott[26], Y. Uchida[26], V. Berardi[27], N. F. Calabria[27], M. G. Catanesi[27], N. Ospina[27], E. Radicioni[27], A. Langella[28], G. De Rosa[28], G. Collazuol[29], M. Feltre[29], M. Mattiazzi[29], L. Ludovici[30], M. Gonin[8], L. Périssé[8], B. Quilain[8], S. Horiuchi[31], A. Kawabata[31], M. Kobayashi[31], Y. M. Liu[31], Y. Maekawa[31], Y. Nishimura[31], R. Akutsu[15], M. Friend[15], T. Hasegawa[15], Y. Hino[15], T. Ishida[15], T. Kobayashi[15], M. Jakkapu[15], T. Matsubara[15], T. Nakadaira[15], Y. Oyama[15], A. Portocarrero Yrey[15], K. Sakashita[15], T. Sekiguchi[15], T. Tsukamoto[15], N. Bhuiyan[32], G. T. Burton[32], F. Di Lodovico[32], J. Gao[32], T. Katori[32], R. Kralik[32], N. Latham[32], R. M. Ramsden[32], H. Ito[33], T. Sone[33], A. T. Suzuki[33], Y. Takeuchi[3,33], S. Wada[33], H. Zhong[33], J. Feng[34], L. Feng[34], S. Han[34], J. Hikida[34], J. R. Hu[34], Z. Hu[34], M. Kawaue[34], T. Kikawa[34], T. V. Ngoc[34], T. Nakaya[3,34], R. A. Wendell[3,34], S. J. Jenkins[35], N. McCauley[35], A. Tarrant[35], M. Fanì[36], M. J. Wilking[36], Z. Xie[36], Y. Fukuda[37], H. Menjo[6,7], Y. Yoshioka[6], J. Lagoda[38], M. Mandal[38], J. Zalipska[38], M. Mori[39], J. Jiang[13], K. Hamaguchi[1], H. Ishino[1], Y. Koshio[1,3], T. Tada[1], T. Ishizuka[40], G. Barr[41], D. Barrow[41], L. Cook[3,41], S. Samani[41], D. Wark[41,42], A. Holin[43], F. Nova[43], S. Jung[44], J. Yoo[44], J. E. P. Fannon[45], L. Kneale[45], M. Malek[45], J. M. McElwee[45], T. Peacock[45], P. Stowell[45], M. D. Thiesse[45], L. F. Thompson[45], H. Okazawa[46], S. M. Lakshmi[47], E. Kwon[48], M. W. Lee[48], J. W. Seo[48], I. Yu[48], Y. Ashida[49], A. K. Ichikawa[49], K. D. Nakamura[49], S. Goto[50], H. Hayasaki[50], S. Kodama[50], Y. Kong[50], Y. Masaki[50], Y. Mizuno[50], T. Muro[50], K. Nakagiri[50], Y. Nakajima[3,50], N. Taniuchi[50], M. Yokoyama[3,50], P. De Perio[3], S. Fujita[3], C. Jesús-Valls[3], K. Martens[3], Ll. Marti[3], K. M. Tsui[3], M. R. Vagins[3,4], J. Xia[3], M. Kuze[51], S. Izumiyama[51], R. Matsumoto[51], R. Asaka[52], M. Ishitsuka[52], M. Sugo[52], M. Wako[52], K. Yamauchi[52], Y. Nakano[53], F. Cormier[34], R. Gaur[11], M. Hartz[11], A. Konaka[11], X. Li[11], B. R. Smithers[11], S. Chen[54], Y. Wu[54], B. D. Xu[54], A. Q. Zhang[54], B. Zhang[54], H. Adhikary[55], M. Girgus[55], P. Govindaraj[55], M. Posiadala-Zezula[55], Y. S. Prabhu[55], S. B. Boyd[56], R. Edwards[56], D. Hadley[56], M. Nicholson[56], M. O'Flaherty[56], B. Richards[56], A. Ali[11,57], B. Jamieson[57], C. Bronner[58], D. Horiguchi[58], A. Minamino[58], Y. Sasaki[58], R. Shibayama[58], and R. Shimamura[58]

The Super-Kamiokande Collaboration

[1] Department of Physics, Okayama University, Okayama, Okayama 700-8530, Japan; nakanishi-suv@s.okayama-u.ac.jp
[2] Kamioka Observatory, Institute for Cosmic Ray Research, University of Tokyo, Kamioka, Gifu 506-1205, Japan
[3] Kavli Institute for the Physics and Mathematics of the Universe (WPI), The University of Tokyo Institutes for Advanced Study, University of Tokyo, Kashiwa, Chiba 277-8583, Japan
[4] Department of Physics and Astronomy, University of California, Irvine, Irvine, CA 92697-4575, USA
[5] Research Center for Cosmic Neutrinos, Institute for Cosmic Ray Research, University of Tokyo, Kashiwa, Chiba 277-8582, Japan
[6] Institute for Space-Earth Environmental Research, Nagoya University, Nagoya, Aichi 464-8602, Japan
[7] Kobayashi-Maskawa Institute for the Origin of Particles and the Universe, Nagoya University, Nagoya, Aichi 464-8602, Japan
[8] ILANCE, CNRS—University of Tokyo International Research Laboratory, Kashiwa, Chiba 277-8582, Japan
[9] Department of Theoretical Physics, University Autonoma Madrid, 28049 Madrid, Spain
[10] Department of Physics, British Columbia Institute of Technology, Burnaby, BC, V5G 3H2, Canada
[11] TRIUMF, 4004 Wesbrook Mall, Vancouver, BC, V6T2A3, Canada
[12] Science Department, Borough of Manhattan Community College/City University of New York, New York, NY 1007, USA
[13] Department of Physics and Astronomy, State University of New York at Stony Brook, NY 11794-3800, USA
[14] Department of Physics, Boston University, Boston, MA 02215, USA
[15] High Energy Accelerator Research Organization (KEK), Tsukuba, Ibaraki 305-0801, Japan
[16] Department of Physics, California State University, Dominguez Hills, Carson, CA 90747, USA
[17] Institute for Universe and Elementary Particles, Chonnam National University, Gwangju 61186, Republic of Korea
[18] Department of Physics, Duke University, Durham, NC 27708, USA
[19] Ecole Polytechnique, IN2P3-CNRS, Laboratoire Leprince-Ringuet, F-91120 Palaiseau, France
[20] Department of Physics, Gifu University, Gifu, Gifu 501-1193, Japan
[21] GIST College, Gwangju Institute of Science and Technology, Gwangju 500-712, Republic of Korea
[22] School of Physics and Astronomy, University of Glasgow, Glasgow, G12 8QQ, UK
[23] Department of Physics and Astronomy, University of Hawaii, Honolulu, HI 96822, USA
[24] Center for Underground Physics, Institute for Basic Science (IBS), Daejeon, 34126, Republic of Korea
[25] Institute For Interdisciplinary Research in Science and Education, ICISE, Quy Nhon, 55121, Vietnam

[26] Department of Physics, Imperial College London, London, SW7 2AZ, UK
[27] Dipartimento Interuniversitario di Fisica, INFN Sezione di Bari and Università e Politecnico di Bari, I-70125, Bari, Italy
[28] Dipartimento di Fisica, INFN Sezione di Napoli and Università di Napoli, I-80126, Napoli, Italy
[29] Dipartimento di Fisica, INFN Sezione di Padova and Università di Padova, I-35131, Padova, Italy
[30] INFN Sezione di Roma and Università di Roma "La Sapienza," I-00185, Roma, Italy
[31] Department of Physics, Keio University, Yokohama, Kanagawa, 223-8522, Japan
[32] Department of Physics, King's College London, London, WC2R 2LS, UK
[33] Department of Physics, Kobe University, Kobe, Hyogo 657-8501, Japan
[34] Department of Physics, Kyoto University, Kyoto, Kyoto 606-8502, Japan
[35] Department of Physics, University of Liverpool, Liverpool, L69 7ZE, UK
[36] School of Physics and Astronomy, University of Minnesota, Minneapolis, MN 55455, USA
[37] Department of Physics, Miyagi University of Education, Sendai, Miyagi 980-0845, Japan
[38] National Centre For Nuclear Research, 02-093 Warsaw, Poland
[39] National Institute of Technology, Numazu College, Numazu 410-8501, Japan
[40] Media Communication Center, Osaka Electro-Communication University, Neyagawa, Osaka, 572-8530, Japan
[41] Department of Physics, Oxford University, Oxford, OX1 3PU, UK
[42] STFC, Rutherford Appleton Laboratory, Harwell Oxford, and Daresbury Laboratory, Warrington, OX11 0QX, UK
[43] Rutherford Appleton Laboratory, Harwell, Oxford, OX11 0QX, UK
[44] Department of Physics and Astronomy, Seoul National University, Seoul 151-742, Republic of Korea
[45] School of Mathematical and Physical Sciences, University of Sheffield, Sheffield, S3 7RH, UK
[46] Department of Informatics in Social Welfare, Shizuoka University of Welfare, Yaizu, Shizuoka, 425-8611, Japan
[47] August Chełkowski Institute of Physics, University of Silesia in Katowice, 75 Pułku Piechoty 1, 41-500 Chorzów, Poland
[48] Department of Physics, Sungkyunkwan University, Suwon 440-746, Republic of Korea
[49] Department of Physics, Faculty of Science, Tohoku University, Sendai, Miyagi, 980-8578, Japan
[50] Department of Physics, University of Tokyo, Bunkyo, Tokyo 113-0033, Japan
[51] Department of Physics, Institute of Science Tokyo, Meguro, Tokyo 152-8551, Japan
[52] Department of Physics and Astronomy, Faculty of Science and Technology, Tokyo University of Science, Noda, Chiba 278-8510, Japan
[53] Faculty of Science, University of Toyama, Toyama City, Toyama 930-8555, Japan
[54] Department of Engineering Physics, Tsinghua University, Beijing, 100084, People's Republic of China
[55] Faculty of Physics, University of Warsaw, Warsaw, 02-093, Poland
[56] Department of Physics, University of Warwick, Coventry, CV4 7AL, UK
[57] Department of Physics, University of Winnipeg, MB R3J 3L8, Canada
[58] Department of Physics, Yokohama National University, Yokohama, Kanagawa, 240-8501, Japan

Received 2025 November 5; revised 2025 December 9; accepted 2025 December 12; published 2026 January 13

Abstract

In 2024, a failed supernova (SN) candidate, M31-2014-DS1, was reported in the Andromeda galaxy (M31), located at a distance of approximately 770 kpc. In this Letter, we search for neutrinos from this failed SN using data from Super-Kamiokande (SK). Based on the estimated time of black hole formation inferred from optical and infrared observations, we define a search window for neutrino events in the SK data. Using this window, we develop a dedicated analysis method for failed SNe and apply it to M31-2014-DS1, by conducting a cluster search using the timing and energy information of candidate events. No significant neutrino excess is observed within the search region. Consequently, we place an upper limit on the time-integrated electron antineutrino luminosity from M31-2014-DS1 and discuss its implications for various failed SN models and their neutrino emission characteristics. Despite the 18 MeV threshold adopted to suppress backgrounds, the search remains sufficiently sensitive to constrain the Shen-TM1 equation of state, in a more optimistic emission scenario with progenitor stars of 40 $M_\odot$ and relatively high mean electron-antineutrino energies of about 23.2 MeV, yielding a 90% confidence level upper limit of 1.76×10^{53} erg on the time-integrated electron antineutrino luminosity, moderately above the expected value of 1.35×10^{53} erg.

Unified Astronomy Thesaurus concepts: Core-collapse supernovae (304); Neutrino astronomy (1100); Gravitational collapse (662); Andromeda Galaxy (39)

1. Introduction

In 2024, M31-2014-DS1, a failed supernova (SN) candidate —a stellar death in which the explosion is unsuccessful and the star collapses into a black hole without a bright optical display—was reported in M31 at a distance of about 770 kpc (K. De et al. 2024). The object exhibited a 50% increase in mid-infrared (MIR) flux over a 2 yr period starting in 2014 (E. L. Wright et al. 2010; A. Mainzer et al. 2014), while remaining undetected in optical and near-infrared (NIR) imaging observations as of 2023. The progenitor is estimated to have been a massive hydrogen-depleted supergiant, with an estimated mass of around 20 $M_\odot$, for which models indicate that the explosion may fail (T. Sukhbold et al. 2016). In addition, the radius of the inner shell, which corresponds to the innermost dust shell, was found to decrease more than 1000 days after the initial MIR brightening. Although alternative scenarios such as extreme dust obscuration or a major mass-loss episode cannot be fully excluded, these observations suggest that a black hole was likely formed sometime between 2014 and 2017, and M31-2014-DS1 remains a strong candidate for the failed SN.

In the final stage of stellar evolution, massive stars develop iron cores through successive fusion processes. Stars exceeding 8 $M_\odot$ undergo core collapse, resulting in core-collapse SNe (CCSNe). In an archetypal CCSN the initial implosion rebounds, ejecting the star's outer layers and leaving behind a neutron star. However, in some cases—especially in more massive stars—the shock wave does not revive, due to the infall of the surrounding stellar material. The star then collapses into a black hole, with minimal electromagnetic emission.

Both successful and failed SNe release more than 99% of their gravitational binding energy in the form of neutrinos, making them a powerful probe of stellar core physics (see, e.g., A. Burrows et al. 1987; K. Kotake et al. 2006; K. Nakazato et al. 2013; S. Horiuchi & J. P. Kneller 2018; T. Takiwaki & K. Kotake 2018; H. Nagakura et al. 2021; M. Mori et al. 2021). In the case of a successful SN, the emission of neutrinos is expected to last for several tens of seconds up to about 100 s. The luminosity of neutrinos decreases as they carry away the energy of the proto–neutron star, and it cools down. In contrast, failed SNe are expected to exhibit short-lived neutrino emission, lasting only up to a few seconds. This behavior arises from the formation of a black hole at the core, after which neutrinos can no longer escape. The electron antineutrino luminosity tends to increase only until it is cut off by black hole formation (M. Liebendörfer et al. 2004; T. Kuroda & M. Shibata 2023).

CCSNe are commonly observed in various electromagnetic bands, such as optical and infrared bands, and extensive catalogs of such events are maintained by public databases like the Transient Name Server (A. Gal-Yam 2021) and the Astronomer's Telegram (R. E. Rutledge 1998). SNe occurring within the sensitive range of current neutrino telescopes, which typically extends only to our galaxy, are very rare. The estimated rate is about one every several decades (G. A. Tammann et al. 1994).

In contrast to CCSNe, the confirmed observations of failed SNe are rare, with only a few candidates reported. For instance, a failed SN candidate was identified using the Large Binocular Telescope (LBT; J. M. Hill et al. 2014) data in the survey by J. R. Gerke et al. (2015). The survey monitored 27 galaxies within 10 Mpc over a period of 7 yr, searching for massive stars that disappeared without a bright optical SN. Among the monitored stars, one candidate whose mass is estimated to be 18–25 $M_\odot$ in NGC 6946 showed a steady decline in luminosity and vanished from the first to the last observation. This suggests that it may have experienced a failed SN.

The reported observation on M31-2014-DS1 has drawn attention to the possibility of detecting neutrinos from M31-2014-DS1. The prediction of the expected neutrino emission and comparison of these predictions with observational limits from Super-Kamiokande (SK) are discussed in Y. Suwa et al. (2025). In that study, several nuclear equations of state (EOS) that could produce a few-second neutrino burst without a visible electromagnetic signal are examined to evaluate how the emission depends on neutron star properties and nuclear physics uncertainties. These include Lattimer and Swesty (J. M. Lattimer & D. F. Swesty 1991), Shen (H. Shen et al. 1998, 2020), Togashi (H. Togashi et al. 2017), and SFHo (A. W. Steiner et al. 2013) models. Although the SFHo model is not a purely failed SN scenario, it is included because its neutrino emission satisfies the criteria for the few-second time-window cluster search employed in that study. However, these predictions in Y. Suwa et al. (2025) do not fully take into account aspects of neutrino detection such as signal efficiency and the energy threshold effect.

In this Letter, we present the result of a search for neutrinos from M31-2014-DS1 using data from the SK detector. Section 2 describes the details of SN neutrino observation in SK, and Section 3 explains the analysis method. The results of the present search, including the derived upper limits on the time-integrated electron antineutrino luminosity, are presented in Section 4. Finally, Section 5 summarizes the study and discusses its future prospects.

2. Supernova Neutrino Observation in SK

SN neutrinos have been observed only once, from SN 1987A in the Large Magellanic Cloud. A total of 24 neutrino events were detected by Kamiokande (K. Hirata et al. 1987), Irvine-Michigan-Brookhaven (IMB; R. M. Bionta et al. 1987), and Baksan (E. N. Alexeyev et al. 1988), demonstrating these detectors are highly effective for observing SN neutrinos.

SK is a large water-Cherenkov detector experiment located 1000 m underground in Kamioka, Japan (S. Fukuda et al. 2003). It contains 50,000 tonnes of ultrapure water, of which 22,500 tonnes are used as the fiducial volume. In the present analysis, we use data from the pure-water phase, prior to the addition of gadolinium sulfate (i.e., before the SK-Gd phase; J. F. Beacom & M. R. Vagins 2004; K. Abe et al. 2022). This represents the most stable operation period. The energy threshold is 3.49 MeV of electron kinetic energy (K. Abe et al. 2016a).

SK is highly sensitive to neutrinos from CCSNe in the Milky Way. For a CCSN at a distance of 10 kpc, about $\mathcal{O}(1000)$ inverse beta decay (IBD; $\bar{\nu}_e + p \rightarrow e^+ + n$) events are expected to be observed. In IBD interactions, the prompt positron emits Cherenkov light, while the delayed neutron is captured on a proton, producing a 2.2 MeV gamma ray. However, this delayed signal is often undetectable in the pure-water phase due to the low detection efficiency. Taking into account the detection efficiency, the expected number of detected neutrino events from CCSNe occurring in nearby galaxies (e.g., within 1 Mpc) is significantly reduced to $\mathcal{O}(0.1)$. Since SN neutrinos are emitted over a timescale of several to tens of seconds, the few events expected from such distances would appear as a small cluster of events in the SK data. Therefore, we adopt a time-clustering analysis to search for such event grouping.

SK has conducted several searches for SN burst neutrinos (M. Ikeda et al. 2007; M. Mori et al. 2022). These analyses scanned the full dataset with multiple cluster definitions reflecting theoretically motivated timescales, including the initial collapse and bounce, shock revival, and proto–neutron star cooling. The searches are not directed at known astrophysical objects, but rather aim to identify SNe in a blind manner, including those that might have occurred but remained undetected in optical observations due to dust obscuration. A search of the 2008–2018 dataset likewise found no burst-like clusters (M. Mori et al. 2022). In the present analysis, we specifically applied a cluster search criterion optimized for M31-2014-DS1, as described in Section 3.4, representing a more targeted approach than previous blind searches.

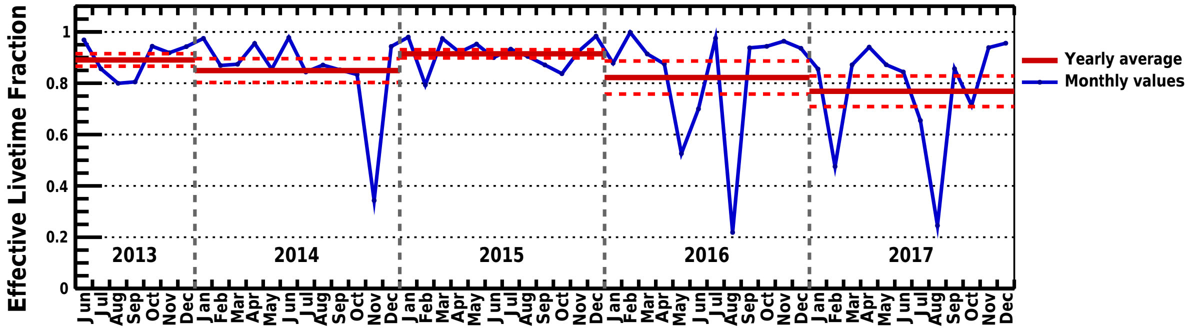

Figure 1. Livetime fraction of SK used in this analysis. The blue line indicates the effective livetime fraction for each month, while the red solid lines show the yearly averaged effective livetime fraction. The red dashed lines represent the standard deviation of the yearly mean. The loss of livetime is mainly attributed to detector calibrations and maintenance periods.

Table 1
Definition of the Signal and Background Time Ranges

Time Range	Period	Duration (days)
Signal time range	2013 Jun 1–2017 Dec 31	1416.3
Background time range (before)	2012 Mar 15–2013 Jun 1	390.5
Background time range (after)	2018 Jan 1–2018 May 31	118.1

3. Analysis Method

We performed a time-clustering analysis of SK data to search for neutrino signals potentially associated with the failed SN candidate M31-2014-DS1. Since SN neutrinos are emitted over a timescale of a few seconds, a signal from M31 would likely appear as a small cluster of temporally correlated events. We defined a 10 s time window and cluster criteria, and then evaluated the expected background to determine the optimal energy threshold. The 10 s window is motivated by numerical simulations of failed SNe, which predict black hole formation within a few seconds after core bounce. At the distance of M31, the expected number of detected neutrinos in SK is $\mathcal{O}(1)$. The estimated background rate corresponds to approximately 1×10^{-5} events per 10 s window above the 18 MeV threshold, indicating that the observation of two or more events within such a time window would represent a statistically significant excess over background expectations. The event selection applied in this search is described in Section 3.4.

3.1. Determination of the Search Region

The exact determination of black hole formation time is difficult with optical telescope observations, because the stellar core where the black hole forms is not directly visible due to the surrounding stellar envelope. Therefore, we defined the "signal time range" as the period fully encompassing the expected time frame for black hole formation, and the "background time range" as the periods immediately before and after it to estimate the background rate. The details are summarized in Table 1. The effective livetime fraction during the signal time range was evaluated. Although the possibility that the SK data were unavailable at the time of the M31-2014-DS1 event (e.g., due to calibration or maintenance periods) cannot be completely excluded, the yearly averaged livetime efficiencies were evaluated as shown in Figure 1. The efficiencies were 89.1% ± 2.4%, 84.9% ± 4.6%, 91.5% ± 1.6%, 82.2% ± 6.4%, and 76.8% ± 6.0% for 2013, 2014, 2015, 2016, and 2017, respectively, indicating that the detector was generally operational during this period. For the background time range, the efficiency were evaluated to be 88.2% ± 3.6% before and 77.4% ± 3.1% after the signal time range.

The presignal background time range is defined as the interval following a known SN candidate, SN 2012aw, observed in 2012 March (D. Poznanski et al. 2012), and extending up to the beginning of the signal time range. The postsignal background time range is defined until the end of the pure-water phase after the signal time range.

3.2. Event Selection

The IBD reaction is the target of the diffuse SN neutrino background (DSNB) search in the neutrino detector; therefore, the event selection and reconstruction follow the previous DSNB search in the pure-water phase (K. Abe et al. 2021). The event selection requires a reconstructed electron or positron total energy above 8 MeV to avoid entering radioactive background events into the data sample. However, to secure the signal event, we did not apply neutron tagging in this search.

In SK, the main background events in the SN neutrino energy region are radio impurities, spallation events, decay electrons from muons, and atmospheric neutrinos. In the case of radio impurities, backgrounds mainly originate from the radio impurities dissolved in purified water (Y. Nakano et al. 2020), the material of the detector structure, and the surrounding rock of the SK tank. Such backgrounds can be reduced by a fiducial volume cut, which excludes events occurring within 2 m of the tank wall. As a result, the tank volume is reduced from the entire inner detector volume of 32,500 tonnes to 22,500 tonnes.

A "spallation event" originates from the decays of unstable isotopes produced when atmospheric muons interact with oxygen nuclei in water (S. W. Li & J. F. Beacom 2014, 2015a, 2015b). The primary spallation process generates hadrons such as pions and neutrons, while the subsequent nuclear interactions produce a variety of beta decay nuclei. The final observables, including beta and gamma rays, have energies from a few MeV up to ~20 MeV. Such spallation events are removed by a spallation cut, which considers pairs of two low-energy events passing the preselection, including information on muons that precede low-energy events within 30 s (S. Locke et al. 2024; Y. Zhang et al. 2016). An additional cut removes events within 4 m and 60 s of another low-energy event, to suppress correlated spallation backgrounds. Details can be found in K. Abe et al. (2021).

The dominant background above 20 MeV originates from charged-current quasi-elastic (CCQE) interactions of atmospheric neutrinos. However, constraints on the CCQE event rate are limited by statistics in the background time range, making it difficult to estimate the background events. Therefore, as described in the next section, we estimated the CCQE background using a simulation.

3.3. Background Event Estimation

To reliably estimate the background rate, we use an atmospheric neutrino Monte Carlo (MC) simulation corresponding to 500 yr based on the HKKM 2011 atmospheric neutrino flux (M. Honda et al. 2007, 2011) and the NEUT 5.3.6 neutrino interaction simulator (Y. Hayato 2009). The flux of atmospheric neutrino CCQE events in the simulation is normalized by fitting the reconstructed energy spectrum in the range $30 < E_{\rm rec} < 60$ MeV to the data. The fit employed the full ~10 yr dataset, including the signal time range, in order to ensure sufficient statistics. Although the signal time range is included, this energy region is above the typical expected neutrino energies from failed SN, and even if a few signal events were present, their contribution to the spectrum would be negligible.

As a result, the estimated background rate is 10.58 day^{-1} for 8 MeV $< E_{\rm rec} \leqslant$ 80 MeV and 0.09 day^{-1} for 18 MeV $< E_{\rm rec} \leqslant$ 80 MeV.

3.4. Evaluation of Background Cluster

To determine the optimal positron energy threshold for the cluster search, we estimate the background event rate and probability of background-induced clusters. The total background estimate consists of two components: (1) a data-driven component estimated by the background in SK below 20 MeV during the background time range, as summarized in Table 1, and (2) an MC-based atmospheric neutrino background above 20 MeV, as described in Section 3.3. We calculated the cluster probability using a toy MC approach. For each energy threshold, we simulated 10^7 trials, where background events are randomly distributed according to the estimated rate. The background events are expected to follow a nearly random distribution. Although some correlation between atmospheric neutrinos and spallation products may exist due to their association with atmospheric muons, such effects are not expected to significantly impact the results of this study. In each trial, we searched for clusters defined as ⩾2 events within a 10 s window, and counted the number of such occurrences. The cluster probability is defined as the fraction of trials that contain at least one cluster:

$$P = \frac{N_{\geqslant 1\ \rm cluster}}{N_{\rm trials}}, \quad (1)$$

where $N_{\geqslant 1\ \rm cluster}$ is the number of trials with one or more clusters, and $N_{\rm trials}$ is the total number of trials. We require the probability to be below the 3σ level ($P < 0.003$), ensuring that any observed cluster is not likely to be due to statistical fluctuations of the background. As shown in Figure 2, the cluster probability decreases with increasing energy threshold. Based on this evaluation, we set the energy threshold to 18 MeV, which satisfies the 3σ criterion. At this threshold, the observation of two or more events within 10 s would constitute a detection.

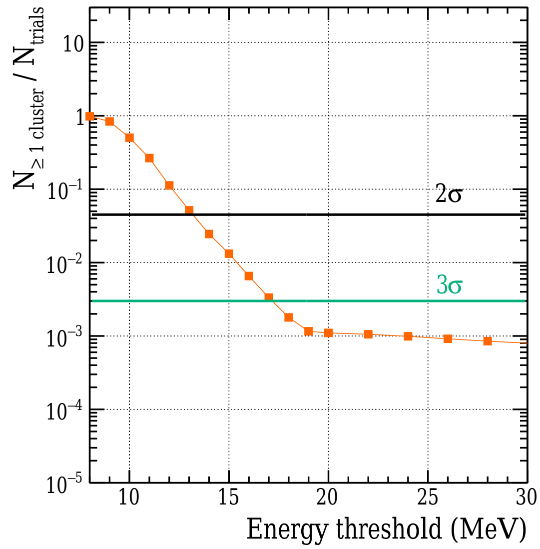

Figure 2. The expected probability of observing clusters due to background events at each energy threshold. The red points indicate the probability of observing one or more clusters within the signal time range. The black and green lines represent the fractions of trials without any clusters at the 2σ and 3σ levels, respectively.

4. Result

Following the cluster search procedure, no clusters consisting of two or more events within a 10 s window were found in the signal time range.

Based on this result, we set the upper limit on the time-integrated electron antineutrino luminosity ($L_{\bar{\nu}_e}$) using two complementary methods. In both methods, the expected number of signal events in SK is estimated by taking into account the detector response and signal efficiency.

In the first approach, we derive an upper limit on the $L_{\bar{\nu}_e}$ by calculating the 90% confidence level (CL) upper limit on the neutrino fluence at SK, based on the assumption of specific failed SN models. The fluence upper limit is calculated as (K. Abe et al. 2016b)

$$\Phi = \frac{N_{90}}{N_T \int dE_{\bar{\nu}_e}\, \lambda(E_{\bar{\nu}_e})\sigma(E_{\bar{\nu}_e})R(E_e, E_{\rm vis})\epsilon(E_{\rm vis})}. \quad (2)$$

Here, Φ is the upper limit on the neutrino fluence. N_{90}, E_e, and $E_{\rm vis}$ represent the 90% CL upper limit on the number of neutrino events in the search window, the true electron energy, and the reconstructed visible energy, respectively. Since no clusters are observed within a 10 s time window, we set $N_{90} = 3.89$, based on the probability to observe at least two events. N_T is the number of target particles in the detector. $\lambda(E_{\bar{\nu}_e})$ denotes the normalized neutrino energy spectrum, $\sigma(E_{\bar{\nu}_e})$ is the neutrino interaction cross section from Strumia–Vissani model (A. Strumia & F. Vissani 2003), $R(E_e, E_{\rm vis})$ is the energy response function that connects E_e to $E_{\rm vis}$, and $\epsilon(E_{\rm vis})$ is the detection efficiency as a function of visible energy. The effect of $R(E_e, E_{\rm vis})$ is expected to be small in the energy range relevant to this analysis, and is therefore not taken into account in this analysis. Using the fluence upper limit Φ, we derive a corresponding upper limit on $L_{\bar{\nu}_e}$ under the

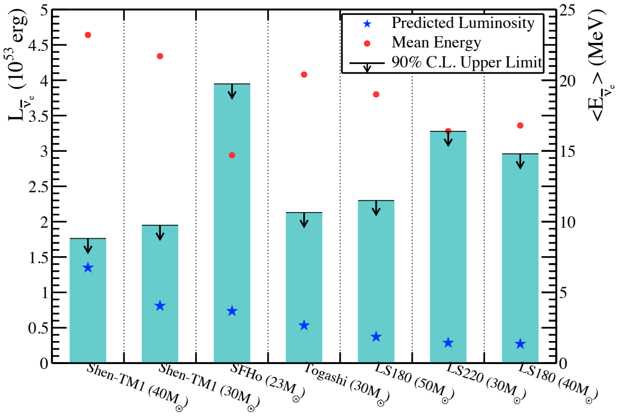

Figure 3. Upper limits on the time-integrated electron antineutrino luminosity ($L_{\bar{\nu}_e}$) for each failed SN model. The models are arranged from left to right in order of decreasing predicted $L_{\bar{\nu}_e}$. The star marks the predicted $L_{\bar{\nu}_e}$ of the model, while the black downward arrow indicates the 90% CL upper limit obtained in the present work. The circle points show the mean electron antineutrino energy for each model, plotted with the right vertical axis, while the $L_{\bar{\nu}_e}$ is shown with the left axis. The Shen2013TM1 (40 $M_\odot$) model follows K. Sumiyoshi et al. (2007). The Shen2013TM1 (30 $M_\odot$), Togashi (30 $M_\odot$), and LS220 (30 $M_\odot$) models are taken from K. Nakazato et al. (2021). The SFHo (23 $M_\odot$) model is adopted from L. Choi et al. (2025), and the LS180 (40 $M_\odot$) and LS180 (50 $M_\odot$) models follow K. Sumiyoshi et al. (2008).

assumption of isotropic emission. The relation is given by

$$L_{\bar{\nu}_e} = 4\pi D^2 \langle E_{\bar{\nu}_e} \rangle \cdot \Phi, \quad (3)$$

where $D = 770$ kpc and $\langle E_{\bar{\nu}_e} \rangle = \int_0^\infty \lambda(E) dE$ is the mean energy of the emitted electron antineutrinos based on the failed SN model spectrum (K. Nakazato et al. 2021; K. Sumiyoshi et al. 2007, 2008; L. Choi et al. 2025). Although neutrinos of all flavors are emitted in a CCSN, only the detectable electron antineutrinos are taken into account in this calculation. In Figure 3, the upper limits of $L_{\bar{\nu}_e}$ for each failed SN model are shown. For models that predict both high $L_{\bar{\nu}_e}$ and higher mean neutrino energy, such as 40 $M_\odot$ simulations using Shen-TM1 in K. Sumiyoshi et al. (2007), the upper limit derived from our analysis approaches the predicted $L_{\bar{\nu}_e}$. In contrast, for models like SFHo (23 $M_\odot$ L. Choi et al. 2025), which represent a fallback SN scenario—where the star initially explodes but later experiences substantial late-time fallback leading to black hole formation—the lower mean neutrino energy makes the fluence upper limit more sensitive to the analysis energy threshold.

In another approach, we estimated the number of expected events for IBD using a Fermi–Dirac neutrino spectrum characterized by a temperature T and $L_{\bar{\nu}_e}$. The expected number of events is calculated as

$$N_{\text{event}} = \int_{E_{\text{th}}}^{\infty} N_T \cdot \phi(E_{\bar{\nu}_e}) \cdot \sigma(E_{\bar{\nu}_e}) \cdot \epsilon(E_{\bar{\nu}_e}) \cdot dE_{\bar{\nu}_e}. \quad (4)$$

Here, $\phi(E_{\bar{\nu}_e})$ is the neutrino fluence at the Earth, and other variables are the same as Equation (2). $\phi(E_{\bar{\nu}_e})$ is derived from a Fermi–Dirac distribution assuming a T and $L_{\bar{\nu}_e}$, with zero chemical potential. The distribution is normalized to satisfy the condition

$$L_{\bar{\nu}_e} = \int_0^\infty E_{\bar{\nu}_e} \cdot \frac{dN}{dE_{\bar{\nu}_e}} dE_{\bar{\nu}_e}. \quad (5)$$

The distance to the source, D, is assumed to be 770 kpc, and the fluence is given by $\phi(E_{\bar{\nu}_e}) = 1/4\pi D^2 \cdot dN/dE_{\bar{\nu}_e}$. Figure 4 shows the relationship between $L_{\bar{\nu}_e}$ and the mean electron antineutrino energy, $\langle E_{\bar{\nu}_e} \rangle$. The shaded regions represent the excluded parameter space derived from the nondetection of time-clustered events in SK, assuming Poisson statistics. The contours represent CLs of 50%, 68%, 90%, 95%, and 99%, respectively, which translates to a Poisson upper limit of 1.68, 2.35, 3.89, 4.74, and 6.64 events in the search window. Contours indicate combinations of emission parameters $L_{\bar{\nu}_e}$, $\langle E_\nu \rangle$) for which the probability of detecting two or more events would have exceeded the given CL. While the 18 MeV threshold in the cluster search was chosen to reduce the number of backgrounds effectively, the sensitivity remains sufficient to constrain the Shen-TM1 relativistic mean-field EOS, which is relatively stiff and yields a maximum cold neutron star mass of 2.2 $M_\odot$, at a CL exceeding 68%, demonstrating that this method can effectively constrain optimistic black hole formation scenarios.

As a notional future scenario, we consider a detector with a fiducial volume 10 times larger than that of SK, representative of the scale of Hyper-Kamiokande (HK; Hyper-Kamiokande Proto-Collaboration et al. 2018). In this estimation, we adopt the same analysis conditions as in this study, such as the signal efficiency and the positron energy threshold. In Figure 4, the blue dashed line indicates the upper limit at 90% CL based on the Poisson expectation when no clusters are observed. Under this assumption, many failed SN models can be constrained, highlighting the significant discovery potential of future large-scale detectors. We note that more detailed and dedicated studies are being carried out for HK, which will provide a more realistic assessment of its sensitivity.

5. Summary and Future Prospects

We searched for neutrinos from M31-2014-DS1 using SK data. The timing of black hole formation is uncertain, as the inner core is obscured in optical and infrared wavelengths. Accordingly, the search period was defined from 2013 June 1 to 2017 December 31. In this analysis, we developed a cluster search method optimized for M31-2014-DS1, where a failed SN at the distance of M31 is expected to produce a short neutrino burst. A cluster is defined as two or more events within 10 s, and an 18 MeV positron energy threshold was applied to sufficiently reduce backgrounds. This procedure can be applied to other failed SN searches by reoptimizing the energy threshold for the search based on the telescope's observation period and the cluster criteria inferred from the expected number of events at a given distance. In the case of M31-2014-DS1, no cluster satisfying the selection criteria was found in the signal time range.

From the result, we derive upper limits on the $L_{\bar{\nu}_e}$ using two spectral assumptions: failed SN model predictions and a Fermi–Dirac distribution. For failed SN models, the limits depend on the spectral characteristics. Models such as Shen-TM1 (40 $M_\odot$) with high $L_{\bar{\nu}_e}$ and mean energy yield limits close to the predicted energy, whereas models like SFHo (23 $M_\odot$) with lower mean energy are more affected by the 18 MeV threshold, showing larger deviations. In the Fermi–Dirac-based analysis, models with lower mean neutrino energy require higher $L_{\bar{\nu}_e}$ to maintain the same expected number of

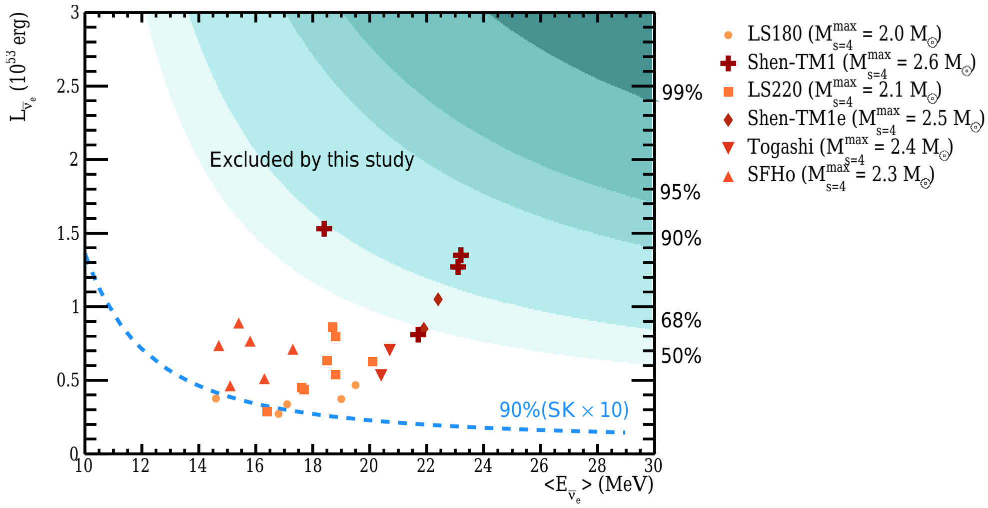

Figure 4. Time-integrated electron antineutrino luminosity $L_{\bar{\nu}_e}$ versus mean energy $\langle E_{\bar{\nu}_e}\rangle$. Shaded regions (light to dark cyan) represent the probability contours (50%, 68%, 90%, 95%, and 99%) for detecting at least two correlated events in SK, based on Poisson statistics for a source located at 770 kpc. The regions above these bands are excluded based on the nondetection of time-clustered events in SK. Filled markers show individual simulation results for six nuclear equations of state (EOS): LS180, LS220, SFHo, Togashi, Shen-TM1e, and Shen-TM1. Each model corresponds to Figure 1 and Table 1 in Y. Suwa et al. (2025). The blue dashed line indicates the 90% probability contour for a detector with 10 times the fiducial mass of SK, assuming Poisson statistics for a source at the distance of 770 kpc.

detected events. As a result, the exclusion contours shift toward higher luminosities as the assumed mean energy decreases. This behavior is reflected in the limit contours shown in Figure 4. Although these contours do not directly provide the numerical limits, the upper limits are evaluated separately under each EOS model assumption as shown in Figure 3. Following this procedure, the search demonstrates sufficient sensitivity to constrain the Shen-TM1 EOS, which represents an optimistic emission scenario based on massive progenitor stars of 40 $M_\odot$ and relatively high mean electron antineutrino energies of 23.2 MeV, resulting in a 90% CL upper limit of 1.76×10^{53} erg on the $L_{\bar{\nu}_e}$, which is moderately above the expected value of 1.35×10^{53} erg.

Improved estimation of the black hole formation time would allow for a narrower signal time range and a lower energy threshold, thereby enhancing the sensitivity to a wider range of failed SN models. In addition, future advances in optical observations may also contribute to narrowing the signal time range. Ongoing optical surveys with facilities such as the LBT and the Subaru Telescope equipped with Hyper Suprime-Cam (S. Miyazaki et al. 2018) already contribute to searches for failed SNe. In the future, the Large Synoptic Survey Telescope (Ž. Ivezić et al. 2019) will extend these efforts with a 10 yr, all-sky time-domain survey. Furthermore, upcoming neutrino detectors such as HK, JUNO (F. An et al. 2016), and DUNE (B. Abi et al. 2020) will offer significantly improved sensitivity to extragalactic failed SNe. These next-generation detectors are expected to detect such events and thereby place much stronger constraints on theoretical models.

Acknowledgments

We gratefully acknowledge the cooperation of the Kamioka Mining and Smelting Company. The Super-Kamiokande experiment has been built and operated from funding by the Japanese Ministry of Education, Culture, Sports, Science and Technology; the US Department of Energy; and the US National Science Foundation. Some of us have been supported by funds from the National Research Foundation of Korea (NRF-2009-0083526, NRF-2022R1A5A1030700, NRF-2022R1A3B1078756, RS-2025-00514948) funded by the Ministry of Science, Information and Communication Technology (ICT); the Institute for Basic Science (IBS-R016-Y2); and the Ministry of Education (2018R1D1A1B07049158, 2021R1I1A1A01042256, RS-2024-00442775); the Japan Society for the Promotion of Science; the National Natural Science Foundation of China under grant No. 12375100; the Spanish Ministry of Science, Universities and Innovation (grant PID2021-124050NB-C31); the Natural Sciences and Engineering Research Council (NSERC) of Canada; the Scinet and Digital Research of Alliance Canada; the National Science Centre (UMO-2018/30/E/ST2/00441 and UMO-2022/46/E/ST2/00336) and the Ministry of Science and Higher Education (2023/WK/04), Poland; the Science and Technology Facilities Council (STFC) and Grid for Particle Physics (GridPP), UK; the European Union's Horizon 2020 Research and Innovation Programme H2020-MSCA-RISE-2018 JENNIFER2 grant agreement No. 822070 and H2020-MSCA-RISE-2019 SK2HK grant agreement No. 872549; the European Union's Next Generation EU/PRTR grant CA3/RSUE2021-00559; and the National Institute for Nuclear Physics (INFN), Italy.

ORCID iDs

F. Nakanishi https://orcid.org/0000-0003-4408-6929
Y. Asaoka https://orcid.org/0000-0001-6440-933X
M. Harada https://orcid.org/0000-0003-3273-946X
Y. Hayato https://orcid.org/0000-0002-8683-5038
K. Hiraide https://orcid.org/0000-0003-1229-9452
K. Hosokawa https://orcid.org/0000-0002-8766-3629
K. Ieki https://orcid.org/0000-0002-7791-5044
M. Ikeda https://orcid.org/0000-0002-4177-5828
Y. Kataoka https://orcid.org/0000-0001-9090-4801
S. Moriyama https://orcid.org/0000-0001-7630-2839
M. Nakahata https://orcid.org/0000-0001-7783-9080
S. Nakayama https://orcid.org/0000-0002-9145-714X
Y. Noguchi https://orcid.org/0000-0002-3113-3127
G. Pronost https://orcid.org/0000-0001-6429-5387
H. Sekiya https://orcid.org/0000-0001-9034-0436

M. Shiozawa https://orcid.org/0000-0003-0520-3520
Y. Takemoto https://orcid.org/0000-0003-2232-7277
T. Yano https://orcid.org/0000-0002-5320-1709
Y. Itow https://orcid.org/0000-0002-8198-1968
K. Okumura https://orcid.org/0000-0002-5523-2808
T. Tashiro https://orcid.org/0000-0003-1440-3049
P. Fernandez https://orcid.org/0000-0001-9034-1930
L. Labarga https://orcid.org/0000-0002-6395-9142
C. Yanagisawa https://orcid.org/0000-0002-6490-1743
E. Kearns https://orcid.org/0000-0002-1781-150X
L. Wan https://orcid.org/0000-0001-5524-6137
T. Wester https://orcid.org/0000-0001-6668-7595
N. J. Griskevich https://orcid.org/0000-0003-4409-3184
H. W. Sobel https://orcid.org/0000-0001-5073-4043
A. Yankelevich https://orcid.org/0000-0002-5963-3123
B. S. Yang https://orcid.org/0000-0001-5877-6096
B. Bodur https://orcid.org/0000-0001-8454-271X
K. Scholberg https://orcid.org/0000-0002-7007-2021
C. W. Walter https://orcid.org/0000-0003-2035-2380
A. Beauchêne https://orcid.org/0000-0001-7781-1483
A. Ershova https://orcid.org/0000-0001-6335-2343
Th. A. Mueller https://orcid.org/0000-0003-2743-4741
P. Paganini https://orcid.org/0000-0001-9580-683X
R. Rogly https://orcid.org/0000-0003-2530-5217
L. N. Machado https://orcid.org/0000-0002-7578-4183
F. J. .P Soler https://orcid.org/0000-0002-4893-3729
N. W. Prouse https://orcid.org/0000-0003-1037-3081
M. Scott https://orcid.org/0000-0002-1759-4453
V. Berardi https://orcid.org/0000-0002-8387-4568
N. F. Calabria https://orcid.org/0000-0003-3590-2808
N. Ospina https://orcid.org/0000-0002-8404-1808
A. Langella https://orcid.org/0000-0001-6273-3558
G. Collazuol https://orcid.org/0000-0002-7876-6124
M. Mattiazzi https://orcid.org/0000-0003-3900-6816
L. Périssé https://orcid.org/0000-0003-3444-4454
Y. Nishimura https://orcid.org/0000-0002-7666-3789
T. Hasegawa https://orcid.org/0000-0002-2967-1954
Y. Hino https://orcid.org/0000-0002-7480-463X
T. Matsubara https://orcid.org/0000-0003-3187-6710
Y. Oyama https://orcid.org/0000-0002-1689-0285
F. Di Lodovico https://orcid.org/0000-0003-3952-2175
T. Katori https://orcid.org/0000-0002-9429-9482
R. M. Ramsden https://orcid.org/0009-0005-3298-6593
H. Ito https://orcid.org/0000-0003-1029-5730
Y. Takeuchi https://orcid.org/0000-0002-4665-2210
S. Han https://orcid.org/0009-0002-8908-6922
J. R. Hu https://orcid.org/0000-0003-2149-9691
Z. Hu https://orcid.org/0000-0002-0353-8792
T. V. Ngoc https://orcid.org/0000-0002-6737-2955
T. Nakaya https://orcid.org/0000-0003-3040-4674
R. A. Wendell https://orcid.org/0000-0002-0969-4681
S. J. Jenkins https://orcid.org/0000-0002-0982-8141
N. McCauley https://orcid.org/0000-0002-5982-5125
A. Tarrant https://orcid.org/0000-0002-8750-4759
M. Fanì https://orcid.org/0000-0002-4284-9614
Z. Xie https://orcid.org/0009-0003-0144-2871
Y. Fukuda https://orcid.org/0000-0003-2660-1958
H. Menjo https://orcid.org/0000-0001-8466-1938
M. Mori https://orcid.org/0000-0002-0827-9152
Y. Koshio https://orcid.org/0000-0003-0437-8505
T. Tada https://orcid.org/0009-0008-8933-0861
D. Barrow https://orcid.org/0000-0001-5844-709X
F. Nova https://orcid.org/0000-0002-0769-9921
S. Jung https://orcid.org/0009-0007-8244-8106
L. Kneale https://orcid.org/0000-0002-4087-1244
M. D. Thiesse https://orcid.org/0000-0002-0775-250X
L. F. Thompson https://orcid.org/0000-0001-6911-4776
E. Kwon https://orcid.org/0000-0001-5653-2880
M. W. Lee https://orcid.org/0009-0009-7652-0153
J. W. Seo https://orcid.org/0000-0002-2719-2079
I. Yu https://orcid.org/0000-0003-1567-5548
Y. Ashida https://orcid.org/0000-0003-4136-2086
A. K. Ichikawa https://orcid.org/0000-0002-1009-1490
K. D. Nakamura https://orcid.org/0000-0003-3302-7325
K. Nakagiri https://orcid.org/0000-0001-8393-1289
Y. Nakajima https://orcid.org/0000-0002-2744-5216
M. Yokoyama https://orcid.org/0000-0003-2742-0251
P. De Perio https://orcid.org/0000-0002-0741-4471
S. Fujita https://orcid.org/0000-0002-0281-2243
C. Jesús-Valls https://orcid.org/0000-0002-0154-2456
K. Martens https://orcid.org/0000-0002-5049-3339
Ll. Marti https://orcid.org/0000-0002-5172-9796
M. R. Vagins https://orcid.org/0000-0002-0569-0480
J. Xia https://orcid.org/0000-0003-1412-092X
M. Kuze https://orcid.org/0000-0001-8858-8440
S. Izumiyama https://orcid.org/0000-0002-0808-8022
R. Matsumoto https://orcid.org/0000-0002-4995-9242
K. Yamauchi https://orcid.org/0009-0000-0112-0619
Y. Nakano https://orcid.org/0000-0003-1572-3888
B. R. Smithers https://orcid.org/0000-0003-1273-985X
S. Chen https://orcid.org/0000-0002-2376-8413
B. D. Xu https://orcid.org/0000-0001-5135-1319
M. Posiadala-Zezula https://orcid.org/0000-0002-5154-5348
C. Bronner https://orcid.org/0000-0001-9555-6033
A. Minamino https://orcid.org/0000-0001-6510-7106

References

Abe, K., Haga, Y., Hayato, Y., et al. 2016a, PhRvD, 94, 052010
Abe, K., Haga, K., Hayato, Y., et al. 2016b, ApJL, 830, L11
Abe, K., Bronner, C., Hayato, Y., et al. 2021, PhRvD, 104, 122002
Abe, K., Bronner, C., Hayato, Y., et al. 2022, NIMPA, 1027, 166248
Abi, B., Acciarri, R., Acero, M. A., et al. 2020, arXiv:2002.03005
Alexeyev, E. N., Alexeyeva, L. N., Krivosheina, I. V., & Volchenko, V. I. 1988, PhLB, 205, 209
An, F., An, G., An, Q., et al. 2016, JPhG, 43, 030401
Beacom, J. F., & Vagins, M. R. 2004, PhRvL, 93, 171101
Bionta, R. M., Blewitt, G., Bratton, C. B., et al. 1987, PhRvL, 58, 1494
Burrows, A., Lattimer, J. M., Mazurek, T. J., & Yahil, A. 1987, Research in Astrophysics: Stellar Collapse and Supernovae Termination Report, State Univ. of New York
Choi, L., Burrows, A., & Vartanyan, D. 2025, PhRvD, 111, 123038
De, K., MacLeod, M., Jencson, J. E., et al. 2024, arXiv:2410.14778
Fukuda, S., Fukuda, Y., Hayakawa, T., et al. 2003, NIMPA, 501, 418
Gal-Yam, A. 2021, AAS Meeting, 237, 423.05
Gerke, J. R., Kochanek, C. S., & Stanek, K. Z. 2015, MNRAS, 450, 3289
Hayato, Y. 2009, AcPPB, 40, 2477
Hill, J. M., Ashby, D. S., Brynnel, J. G., et al. 2014, SPIE, 9145, 914502
Hirata, K., Kajita, T., Koshiba, M., et al. 1987, PhRvL, 58, 1490
Honda, M., Kajita, T., Kasahara, K., & Midorikawa, S. 2011, PhRvD, 83, 123001
Honda, M., Kajita, T., Kasahara, K., Midorikawa, S., & Sanuki, T. 2007, PhRvD, 75, 043006
Horiuchi, S., & Kneller, J. P. 2018, JPhG, 45, 043002
Hyper-Kamiokande Proto-Collaboration, Abe, K., Abe, K., et al. 2018, arXiv:1805.04163
Ikeda, M., Takeda, A., Fukuda, Y., et al. 2007, ApJ, 669, 519
Ivezić, Ž., Kahn, S. M., Tyson, J. A., et al. 2019, ApJ, 873, 111
Kotake, K., Sato, K., & Takahashi, K. 2006, RPPh, 69, 971

Kuroda, T., & Shibata, M. 2023, MNRAS, 526, 152
Lattimer, J. M., & Swesty, D. F. 1991, NuPhA, 535, 331
Li, S. W., & Beacom, J. F. 2014, PhRvC, 89, 045801
Li, S. W., & Beacom, J. F. 2015a, PhRvD, 91, 105005
Li, S. W., & Beacom, J. F. 2015b, PhRvD, 92, 105033
Liebendörfer, M., Messer, O. E. B., Mezzacappa, A., et al. 2004, ApJS, 150, 263
Locke, S., Coffani, A., Abe, K., et al. 2024, PhRvD, 110, 032003
Mainzer, A., Bauer, J., Cutri, R. M., et al. 2014, ApJ, 792, 30
Miyazaki, S., Komiyama, Y., Kawanomoto, S., et al. 2018, PASJ, 70, S1
Mori, M., Abe, K., Hayato, Y., et al. 2022, ApJ, 938, 35
Mori, M., Suwa, Y., Nakazato, K., et al. 2021, PTEP, 2021, 023E01
Nagakura, H., Burrows, A., Vartanyan, D., & Radice, D. 2021, MNRAS, 500, 696
Nakano, Y., Hokama, T., Matsubara, M., et al. 2020, NIMPA, 977, 164297
Nakazato, K., Sumiyoshi, K., Suzuki, H., et al. 2013, ApJS, 205, 2
Nakazato, K., Sumiyoshi, K., & Togashi, H. 2021, PASJ, 73, 639
Poznanski, D., Nugent, P. E., Ofek, E. O., Gal-Yam, A., & Kasliwal, M. M. 2012, ATel, 3996, 1
Rutledge, R. E. 1998, PASP, 110, 754
Shen, H., Ji, F., Hu, J., & Sumiyoshi, K. 2020, ApJ, 891, 148
Shen, H., Toki, H., Oyamatsu, K., & Sumiyoshi, K. 1998, NuPhA, 637, 435
Steiner, A. W., Hempel, M., & Fischer, T. 2013, ApJ, 774, 17
Strumia, A., & Vissani, F. 2003, PhLB, 564, 42
Sukhbold, T., Ertl, T., Woosley, S. E., Brown, J. M., & Janka, H. T. 2016, ApJ, 821, 38
Sumiyoshi, K., Yamada, S., & Suzuki, H. 2007, ApJ, 667, 382
Sumiyoshi, K., Yamada, S., & Suzuki, H. 2008, ApJ, 688, 1176
Suwa, Y., Akaho, R., Ashida, Y., et al. 2025, OJAp, 8, 167
Takiwaki, T., & Kotake, K. 2018, MNRAS, 475, L91
Tammann, G. A., Loeffler, W., & Schroeder, A. 1994, ApJS, 92, 487
Togashi, H., Nakazato, K., Takehara, Y., et al. 2017, NuPhA, 961, 78
Wright, E. L., Eisenhardt, P. R. M., Mainzer, A. K., et al. 2010, AJ, 140, 1868
Zhang, Y., Abe, K., Haga, Y., et al. 2016, PhRvD, 93, 012004